Light scattering from a dense and ultracold atomic gas

I. M. Sokolov, M. D. Kupriyanova, and D. V. Kupriyanov*
Department of Theoretical Physics, State Polytechnic University, 195251 St. Petersburg, Russia

M. D. Havey
Department of Physics, Old Dominion University, Norfolk, Virginia 23529, USA
(Received 3 May 2008; revised manuscript received 18 December 2008; published 7 May 2009)

The quantum optical response of high-density ultracold atomic systems is important to a wide range of fundamentally and technically important physical processes. We present here a microscopic analysis of the light scattering on such a system and compare it with a corresponding description based on macroscopic Maxwell theory. Results are discussed in the context of the spectral resonance structure of the scattering cross section, the time-dependent response under a range of conditions, and evolution of these quantities as the atomic density is varied. For high atomic densities, the microscopic theoretical treatment reveals a distributed and configuration-dependent narrow resonance structure. This structure is attributed to microcavity spatial structures associated with the dense and ultracold atomic gases.

DOI: 10.1103/PhysRevA.79.053405 PACS number(s): 34.50.Rk, 03.67.Mn, 34.80.Qb, 42.50.Ct

I. INTRODUCTION

A significant range of studies of ultracold atomic systems have focused on their quantum degenerate behavior near the Bose-Einstein condensation phase transition [1]. At the same time, a large number of other research areas emerged from studies of ultracold atomic gas samples such as ultracold molecule formation [2], image storage in high-optical depth samples [3], and light storage and manipulation for possible atomic-physics-based quantum repeaters [4] and other quantum information applications. One little explored, but quite broad, area which may have significant impact in a range of scientific or technical areas is the study of quantum optical processes at high density n_0, where $n_0\lambda\!\!\!^{-3} \sim 1$, i.e., for the systems with more than one atom in the volume of cubic wavelength [5]. Under these conditions, disorder-dependent phenomena such as an Anderson-type [6] localization, random lasing [7], and other mesoscopic phenomena [8–10] may appear. In these cases, the high-density quantum optical response of the medium is of critical importance to understanding the dressing and probing of the physical processes involved. In this paper we are concerned with the collective dynamics of light and a sample of ultracold and high-density atoms. Under the conditions that $n_0\lambda\!\!\!^{-3} \gtrsim 1$ the interaction of atomic dipoles via longitudinal and transverse electric fields strongly interferes with the scattering process. The atomic dipoles cannot be considered as independent secondary sources of the scattered waves freely propagating through the sample, as what usually takes place for an optically dilute system. Here we present theoretical discussion of the scattering process based on two different and complementary approaches. In the first, we use a self-consistent description of the atomic sample in the spirit of the Debye-Mie model for a macroscopic spherical scatterer consisting of a homogeneous and dense configuration of atomic dipoles. We apply a self-consistent calculation of the macroscopic permittivity via the relevant statistical description of the polarization response on an external field [11]. Although much of this approach (in a variety of different contexts) appears elsewhere in the literature, it provides a natural base of comparison with more quantum-posed treatments of the light-scattering problem. For this reason, in a second approach we make a numerical analysis of the completely quantum-posed description of the single-photon scattering problem. This analysis gives us the value of the scattering amplitude and, in particular, shows the correct description of the cross section in those spectral domains where the Debye-Mie model fails or is not irreproachably applicable. Our results also suggest the presence of collective microcavity structure created by the atomic system, where a number of resonant modes have a subradiant nature, and discuss their physical substance in the context of light scattering and diffusion. The results may have important implications for studies of atomic physics analogs of light localization, random lasing in an ultracold atomic gas, and for manipulation of single and few photon states in ultracold and dense atomic gases.

II. MACROSCOPIC APPROACH

A. Dielectric permittivity of a dense atomic system

Light transport through a disordered system of atomic dipoles can be discussed in the Maxwell theory as a combination of the process of coherent propagation described by configuration averaged Maxwell equations and incoherent losses initiated by scattering from mesoscopically scaled permittivity fluctuations. In such a formalism one can visualize the light state as a local plane wave existing on a spatial scale $\sim\lambda$ and coherently interacting with the system of atomic dipoles located in a relevant mesoscopic volume. The dipoles interacting with the field are locally indistinguishable and the interaction process is assumed to be well approximated by the cooperative coherent response [11] for the sample susceptibility $\chi(\omega)$ at frequency ω. Below we show how the dielectric susceptibility and permittivity of the homogeneous

*Present address: SPbSU, 198504 St. Petersburg, Russia; kupr@dk11578.spb.edu

medium, built by a system of ultracold atomic dipoles that interact with the environment via radiative channels, can be calculated. Our approach is based on idea of self-consistency, which ignores any possible correlations among the dipoles, but keeps their mutual interferences within the macroscopic dielectric constant of the medium.

The Heisenberg dynamics of the positive frequency component of an ath atomic dipole $\hat{d}_j^{(a,+)}(t)$ $(j=x,y,z,\ a=1-N)$, located at spatial point $\mathbf{r}_a$, is driven by the following equation:

$$\dot{\hat{d}}_j^{(a,+)}(t) = \frac{i}{\hbar}[\hat{H}(t),\hat{d}_j^{(a,+)}(t)] = -i\omega_0\hat{d}_j^{(a,+)}(t) + \frac{i}{\hbar}[\hat{H}_{\text{self}}(t),\hat{d}_j^{(a,+)}(t)] - \frac{i}{\hbar}\sum_{b=1}^{N}[\hat{\mathbf{d}}^{(b)}(t)\hat{\mathbf{E}}(\mathbf{r}_b,t),\hat{d}_j^{(a,+)}(t)], \tag{2.1}$$

where the first term describes the free-dipole dynamics, (ω_0 is the frequency of atomic transition), the second term is the interaction with the self-action Hamiltonian $\hat{H}_{\text{self}}$, and the last term is responsible for the dipole's dynamics driven by the microscopic displacement field, see Ref. [12] for details. The microscopic displacement field can be expressed by a standard expansion in the basis of plane waves

$$\hat{\mathbf{E}}(\mathbf{r},t) \equiv \hat{\mathbf{E}}^{(+)}(\mathbf{r},t) + \hat{\mathbf{E}}^{(-)}(\mathbf{r},t) = \sum_s \left(\frac{2\pi\hbar\omega_s}{\mathcal{V}}\right)^{1/2}[i\mathbf{e}_s a_s(t)e^{i\mathbf{k}_s\mathbf{r}} - i\mathbf{e}_s a_s^{\dagger}(t)e^{-i\mathbf{k}_s\mathbf{r}}] = \hat{\mathbf{E}}_{\perp}(\mathbf{r},t) + \sum_{b=1}^{N}\frac{4\pi}{\mathcal{V}}\sum_s \mathbf{e}_s[\mathbf{e}_s\hat{\mathbf{d}}^{(b)}(t)]e^{i\mathbf{k}_s(\mathbf{r}-\mathbf{r}_b)}. \tag{2.2}$$

Here the frequency components of the displacement field are associated with the annihilation $[\sim a_s(t)]$ and creation $[\sim a_s^{\dagger}(t)]$ parts of this expansion given by the second line. The sum is extended over all the radiation modes and the composite index $s=\mathbf{k}_s,\alpha$ includes the mode wave vector $\mathbf{k} \equiv \mathbf{k}_s$ and its polarization $\alpha=1,2$. For the sake of further convenience the polarization vectors $\mathbf{e}_s \equiv \mathbf{e}_{\mathbf{k}\alpha}$ are assumed to be real. The last line in expression (2.2) constitutes the relation between the microscopic displacement field and the transverse electric field $\hat{\mathbf{E}}_{\perp}(\mathbf{r},t)$, see Ref. [12]. The difference between these field variables is expressed by the contribution of the microscopic polarization. Time dependence of all the considered operator functions can be always divided into positive and negative frequency parts.

The role of the self-action Hamiltonian, considered together with the self-contact interaction [given by the contribution when $b=a$ in the last term of Eq. (2.2)] for the dipole's dynamics is discussed in Appendix A, where we show that for excitation with a weak coherent field the contribution of these terms can be neglected. Then the dynamics of the selected ath dipole can be rewritten in a form when the action of the transverse electric field $\hat{\mathbf{E}}_{\perp}(\mathbf{r},t)$ is separated from the short-range interaction with other dipoles;

$$\dot{\hat{d}}_j^{(a,+)}(t) = -i\omega_0\hat{d}_j^{(a,+)}(t) - \frac{i}{\hbar}[\hat{d}_i^{(a,-)}(t),\hat{d}_j^{(a,+)}(t)] \times \frac{4\pi}{\mathcal{V}}\sum_{b\neq a}^{N}{}'\sum_s e_{si}[\mathbf{e}_s\hat{\mathbf{d}}^{(b)}(t)]e^{i\mathbf{k}_s(\mathbf{r}_a-\mathbf{r}_b)} - \frac{i}{\hbar}\hat{E}_{\perp i}^{(-)}(\mathbf{r}_a,t) \times [\hat{d}_i^{(a,-)}(t),\hat{d}_j^{(a,+)}(t)] - \frac{i}{\hbar}[\hat{d}_i^{(a,-)}(t),\hat{d}_j^{(a,+)}(t)]\hat{E}_{\perp i}^{(+)}(\mathbf{r}_a,t) + \cdots, \tag{2.3}$$

where the dots indicate the contribution of the neglected terms.

Let us consider the basic scenario for macroscopic electrodynamics when the dense system of atomic dipoles, structuring the bulk medium, is excited by an external weak coherent electromagnetic wave. Then each dipole, considered as one of many indistinguishable ones, will respond to the external field and Eq. (2.3) can be self-consistently averaged by reproducing the following dynamics of the dipole's expectation value

$$\langle\dot{\hat{d}}_j^{(a,+)}(t)\rangle = -i\omega_0\langle\hat{d}_j^{(a,+)}(t)\rangle + \frac{i}{\hbar}\frac{|d_{F_0F}|^2}{3(2F_0+1)}\left[\frac{4\pi}{3}\mathcal{P}_j^{(+)}(\mathbf{r}_a,t) + \mathcal{E}_j^{(+)}(\mathbf{r}_a,t)\right] - \frac{i}{\hbar}\langle[\hat{d}_i^{(a,-)}(t),\hat{d}_j^{(a,+)}(t)]\hat{E}_{\perp i}^{(a,+)}(\mathbf{r}_a,t)\rangle, \tag{2.4}$$

where $\mathcal{P}_j^{(+)}(\mathbf{r},t)$ is the mesoscopically averaged polarization, defined below [see Eq. (2.7)] which is considered in Eq. (2.4) at the point of the dipole's location. Here we denoted as $\mathcal{E}_j^{(+)}(\mathbf{r},t)=\langle\hat{E}_{\perp j}^{(+)}(\mathbf{r},t)\rangle$ the jth vector component of the averaged coherent wave of the transverse electric field propagating in the medium.

While deriving Eq. (2.4) from Eq. (2.3) we left only the terms coordinated with the rotating wave approximation (RWA). The short-range interaction with the environment of proximal dipoles is self-consistently approximated by the local-field correction, see Refs. [13–15]. In Eq. (2.4) the expectation value of the atomic dipole $\langle\hat{d}_j^{(a,+)}(t)\rangle$ reveals a coherent response to the driving field and, in an isotropic environment, this coincides with the direction of the electric field $\mathcal{E}_j^{(+)}(\mathbf{r},t)$. It is important to recognize that while transforming the exact microscopic dipole's dynamics to its macroscopic description we ignored all possible correlation effects in the atomic system, which is a standard simplification of the self-consistent approximation. Thus we will further assume that the system of atomic dipoles creates a collective material wave responding to and driven by the field wave $\mathcal{E}_j^{(+)}(\mathbf{r},t)$ via the macroscopic susceptibility of the medium.

The last term in Eq. (2.4) describes the influence of the incoherently reradiated field $\hat{E}_{\perp i}^{(a,+)}(\mathbf{r}_a,t)$ of the ath dipole on its own dynamics, which is responsible for the damping of coherent propagation of the driving wave. This field is given by a solution of the macroscopic Maxwell Equations, where the selected dipole is considered as a pointlike source, and the last term in Eq. (2.4) can be expressed as follows:

$$\langle[\hat{d}_i^{(a,-)}(t),\hat{d}_j^{(a,+)}(t)]\hat{E}_{\perp i}^{(a,+)}(\mathbf{r}_a,t)\rangle = \int_{-\infty}^{t} dt' D_{il}^{(R)}(\mathbf{0},t-t') \times \left\langle [\hat{d}_i^{(a,-)}(t),\hat{d}_j^{(a,+)}(t)]\frac{1}{\hbar c^2}\frac{\partial^2}{\partial t'^2}\hat{d}_l^{(a,+)}(t')\right\rangle, \tag{2.5}$$

where

$$D_{il}^{(R)}(\mathbf{R},\tau) = -\int_{-\infty}^{\infty}\frac{d\omega}{2\pi}e^{-i\omega\tau}\int\frac{d^3k}{(2\pi)^3}e^{i\mathbf{k}\cdot\mathbf{R}}\frac{4\pi\hbar}{k^2-\epsilon(\omega)\frac{\omega^2}{c^2}} \times\left[\delta_{il}-\frac{k_i k_l}{k^2}\right] \tag{2.6}$$

is the retarded type Green's function of the macroscopic Maxwell Equations in the homogeneous medium, see Ref. [11]. It is crucial in evaluation of integral (2.5) that the retardation effect can be ignored in the dipole's dynamics for the time increment $\tau=t-t'$ and the algebraic relations for the atomic Heisenberg operators can be considered the same as for the coincident time arguments. The nonconverging part of the integral is connected with the spectral wings of the integrand and can be regularized by subtracting the similar contribution of the nonconverging Lamb shift, such that ω_0 should be further associated with the physical transition frequency of an isolated atom.

Let us introduce the mesoscopically averaged atomic polarization

$$\mathcal{P}_j^{(+)}(\mathbf{r},t) = \frac{1}{\Delta V}\sum_{a\in\Delta V}\langle\hat{d}_j^{(a,+)}(t)\rangle, \tag{2.7}$$

where the sum is extended over the atoms located inside a small mesoscopic volume ΔV near the point $\mathbf{r}$, and it is assumed that all the dipoles are indistinguishable and have identical time dynamics. While applying Eq. (2.7) one makes a configuration average over random locations of atomic dipoles and smooths the description to the macroscopic approach. For the system of isotropic atomic scatterers, such mesoscopically averaged atomic polarization is described by a coherent transverse matter wave copropagating with the driving field. Then one arrives at the following self-consistent equation for the Fourier component of the atomic polarization:

$$-i\omega\mathcal{P}_j^{(+)}(\mathbf{r},\omega) = -i\left(\omega_0-\frac{4\pi n_0}{3\hbar}\frac{|d_{F_0F}|^2}{3(2F_0+1)}\right)\mathcal{P}_j^{(+)}(\mathbf{r},\omega) + in_0\frac{|d_{F_0F}|^2}{3\hbar(2F_0+1)}\mathcal{E}_j^{(+)}(\mathbf{r},\omega) - \frac{1}{2}\sqrt{\epsilon(\omega)}\gamma \times\mathcal{P}_j^{(+)}(\mathbf{r},\omega), \tag{2.8}$$

where n_0 is the average density of atoms, d_{F_0F} is the reduced matrix element for the dipole moment between the lower and upper states with angular momenta F_0 and F, respectively, and γ is the natural radiation rate for an isolated atom.

This equation gives the spectral response of the atomic polarization to the averaged field in the medium $\mathcal{P}_j^{(+)}(\mathbf{r},\omega)=\chi(\omega)\mathcal{E}_j^{(+)}(\mathbf{r},\omega)$. Hence, the dielectric permittivity $\epsilon(\omega)=1+4\pi\chi(\omega)$ can be extracted via a self-consistent approximation of the collective dipole dynamics driven by the transverse electric field and modified by the Lorentz-Lorenz effect. Thus, if incoherent losses have only a radiative nature and atoms equally populate the ground-state Zeeman sublevels, we obtain the following self-consistent expression for $\epsilon(\omega)$ for an infinite sample:

$$\epsilon(\omega) = \left[1-\frac{8\pi n_0}{3\hbar}\frac{|d_{F_0F}|^2}{3(2F_0+1)}\frac{1}{\omega-\omega_0+i\sqrt{\epsilon(\omega)}\gamma/2}\right] \times\left[1+\frac{4\pi n_0}{3\hbar}\frac{|d_{F_0F}|^2}{3(2F_0+1)}\frac{1}{\omega-\omega_0+i\sqrt{\epsilon(\omega)}\gamma/2}\right]^{-1}. \tag{2.9}$$

As follows from the above derivation the macroscopic correction of the radiative decay $\sqrt{\epsilon(\omega)}\gamma/2$ is built by the self-energy operator for an internal atomic dipole radiating in the medium via the dressed photon Green's function [Eq. (2.6)]. This dipole contributes to the mesoscopically averaged polarization and is considered as one of many indistinguishable ones belonging to the medium and undergoing the same coherent excitation. This correction should not be confused with the decay constant for an external dipole positioned in the sample, which has been the subject of various discussions [16,17].

The next important point is that the dynamics of the polarization, driven by the external coherent field and considered in the self-consistent model, ignores any correlations induced by recurrent scattering. These effects, which intrinsically have a quantum nature and form the background of the discussions of localization phenomenon [18], are included in our microscopic analysis given below. Equation (2.9) can be analytically solved and $\epsilon(\omega)=\epsilon'(\omega)+i\epsilon''(\omega)$ expressed in terms of well-defined external parameters, such as the natural decay rate γ and density of atoms n_0. The reduced matrix element d_{F_0F} for a given dipole transition can be also expressed in terms of γ. We consider here a closed transition, such that for hyperfine levels only the selected lower and upper states with angular momenta F_0 and F, respectively, are radiatively coupled.

B. Energy conservation and causality

In this section we briefly discuss connections of the previous developments with energy conservation and causality in the physical system considered here. Imagine a coherent wave propagating in the medium as a monochromatic excitation in a certain polarization mode such that

$$\mathcal{E}^{(+)}(\mathbf{r},t) = \mathcal{E}_0(\mathbf{r})e^{-i\omega t}, \tag{2.10}$$

where we omitted the polarization index. Let us introduce the mesoscopically averaged density of the excited atoms $\mathcal{N}(\mathbf{r},t)$ at a spatial point $\mathbf{r}$ and a moment of time t;

$$\mathcal{N}(\mathbf{r},t) = \frac{1}{\Delta V}\sum_{a\in\Delta V}\sum_n\langle|n\rangle\langle n|^{(a)}(t)\rangle, \tag{2.11}$$

where $|n\rangle\langle n|^{(a)}(t)$ is the Heisenberg projector on a nth quantum state of the ath excited atom. The internal averaging

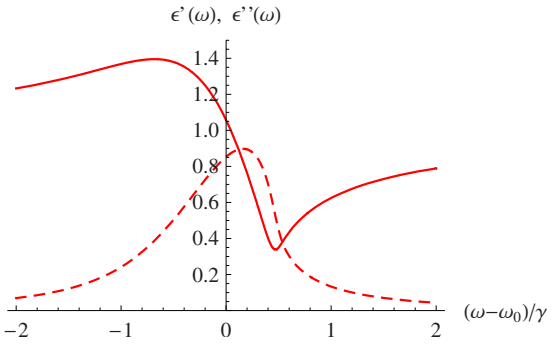

FIG. 1. (Color online) Real (solid) and imaginary (dashed) parts of the dielectric permittivity for the sample with the scaled density $n_0\lambda\!\!\!^{-3}(2F+1)/[3(2F_0+1)]=0.05$. The origin of the plot corresponds to the atomic resonance and the frequency ω is scaled by the natural decay rate γ.

gives an expectation value for a particular configuration, and then we apply the configuration averaging similar to Eq. (2.7).

The dynamics of $\mathcal{N}(\mathbf{r},t)$ can be described in a similar way to how we treated the dipole's polarization in the previous subsection. The rate of the excitations is then given by

$$\dot{\mathcal{N}}(\mathbf{r},t)=\frac{\epsilon''(\omega)}{2\pi\hbar}|\mathcal{E}_0(\mathbf{r})|^2. \tag{2.12}$$

This can be compared with the energy of the wave dissipated by the homogeneous medium in a unit volume per unit time, which is given by the following well-known result of macroscopic electrodynamics, see Ref. [11],

$$\mathcal{Q}(\mathbf{r})=\omega\frac{\epsilon''(\omega)}{2\pi}|\mathcal{E}_0(\mathbf{r})|^2. \tag{2.13}$$

The balance $\mathcal{Q}(\mathbf{r})=\hbar\omega\dot{\mathcal{N}}(\mathbf{r},t)$ clearly indicates that there are no actual losses in such medium. The dissipated energy is instead associated with the energy of the secondary and multiply scattered waves, which further emerge from the medium via diffuse channels.

In Figs. 1 and 2 there are shown two typical spectral dependencies of the dielectric constant plotted for two different densities. The first graph shows the normal analytical behavior responsible for refraction and (conventional) "absorption" processes in the scattering sample. As was verified

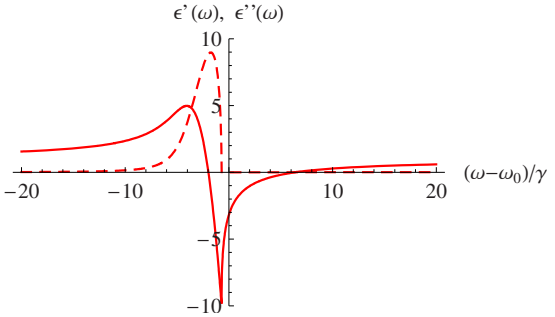

FIG. 2. (Color online) Same as in Fig. 1 but for the density $n_0\lambda\!\!\!^{-3}(2F+1)/[3(2F_0+1)]=1$.

$\epsilon''(\omega)$ describes the losses of that part of the light, which further emerges the sample via channel of incoherent scattering. The absorption resonance is shifted to the blue side of the atomic line because of the radiation correction of the light shift, which exists in the self-consistent model. For low densities this effect manifests itself as more important than the correction associated with the local field. At high densities (see, for example, Fig. 2), there is a spectral domain where $\epsilon'(\omega)<0$ and $\epsilon''(\omega)=0$. Such behavior of the dielectric constant is a well-known effect in classical electrodynamics, see Ref. [11]. It describes a medium where the polarization response is in opposite phase to the external driving field such that the field actually does not penetrate the medium but propagates as a surface wave (surface polariton). For such a medium it is typical that the losses are small and $\epsilon''(\omega)$ is small or even zero. We can emphasize that in the discussed case the vanishing of $\epsilon''(\omega)$ is in accordance with the assumptions made, which exclude nonradiative losses in the system.

As is known, the spectral and analytical behavior of the permittivity should be constrained by the principle of causality. The real and imaginary parts of $\epsilon(\omega)$ are then not independent but instead obey the Kramers-Kronig causality relations. These relations are always fulfilled in any medium as far as there is a causal response of the atomic polarization to the external field, which entirely assumes a certain wave-type solution of the macroscopic Maxwell Equations. In our situation such a wave-type solution does exist at any density. The appearance of negative $\epsilon'(\omega)$ does not eliminate a wave-type solution, it only indicates that a polaritonic type of wave can propagate along the surface and cannot penetrate inside the medium. We have verified that the Kramers-Kronig relations are always fulfilled at any densities for the situation of Eq. (2.9).

C. Light scattering by a uniform density spherical sample

The above results can be applied to calculation of the scattering cross section of light by a uniform density spherical sample of large radius $a(a\gg\lambda\!\!\!^{-}=c/\omega_0)$ in the standard formalism of the Debye-Mie problem,

$$Q_S=\frac{\pi c^2}{2\omega^2}\sum_{J=1}^{\infty}(2J+1)[|1-S_J^{(e)}|^2+|1-S_J^{(m)}|^2],$$

$$Q_A=\frac{\pi c^2}{2\omega^2}\sum_{J=1}^{\infty}(2J+1)[1-|S_J^{(e)}|^2+1-|S_J^{(m)}|^2], \tag{2.14}$$

where the scattering matrix components for the TM and TE modes are, respectively, given by

$$S_J^{(e)}=S_J^{(e)}(\omega)$$
$$=-\frac{\epsilon(\omega)j_J(ka)\left[rh_J^{(2)}\left(\frac{\omega}{c}r\right)\right]'_{r=a}-h_J^{(2)}\left(\frac{\omega}{c}a\right)[rj_J(kr)]'_{r=a}}{\epsilon(\omega)j_J(ka)\left[rh_J^{(1)}\left(\frac{\omega}{c}r\right)\right]'_{r=a}-h_J^{(1)}\left(\frac{\omega}{c}a\right)[rj_J(kr)]'_{r=a}},$$

$$S_J^{(m)} = S_J^{(m)}(\omega) = -\frac{j_J(ka)\left[rh_J^{(2)}\left(\frac{\omega}{c}r\right)\right]'_{r=a} - h_J^{(2)}\left(\frac{\omega}{c}a\right)[rj_J(kr)]'_{r=a}}{j_J(ka)\left[rh_J^{(1)}\left(\frac{\omega}{c}r\right)\right]'_{r=a} - h_J^{(1)}\left(\frac{\omega}{c}a\right)[rj_J(kr)]'_{r=a}}. \quad (2.15)$$

Here $j_J(\cdots)$, $h_J^{(1)}(\cdots)$, and $h_J^{(2)}(\cdots)$ are spherical Bessel functions of Jth order, and $k=k(\omega)=\sqrt{\epsilon(\omega)}\omega/c$. $Q_S=Q_S(\omega)$ is the elastic part of the cross section responsible for the coherent scattering of light from the sample boundary. The absorption part $Q_A=Q_A(\omega)$ is a source for diffusely scattered light via the incoherent channels and the sum $Q_0=Q_0(\omega)=Q_S(\omega)+Q_A(\omega)$ is the total cross section for the entire scattering process. The "absorbed" light emerges from the sample via incoherent channels and the relevant outgoing flux can be recovered in the Maxwell theory by considering secondary and multiply scattered waves generated by fluctuations of $\chi(\omega)$. The analysis of the transient process and time dependence of the fluorescence can be simplified by a diffuse approximation if the extinction length for the field penetration inside the sample is much longer than λ.

Let us point out that while considering the multiply scattered waves, created by random spatial inhomogeneities, the Maxwell theory would restrict such a Monte Carlo analysis by a fluctuation scale much longer than the radiation wavelength. For fine-resolved fluctuations, when the microscopic structure of the system becomes crucially important, one can expect more subtle interaction among proximal dipoles, which includes quantum correlations and recurrent interaction diagrams. This situation can be properly described only via exact microscopic analysis of the problem.

III. MICROSCOPIC APPROACH

With reference to Eq. (2.1) and Appendix A, we now turn to the quantum-posed description of the photon scattering problem. In this treatment, photon scattering on an atomic system is expressed by the following relation between the total cross section and the T-matrix:

$$Q_0 = \frac{\mathcal{V}^2}{\hbar^2 c^4}\frac{\omega'^2}{(2\pi)^2}\int \sum_{\mathbf{e}'} |T_{g\mathbf{e}'\mathbf{k}',g\mathbf{e}\mathbf{k}}(E_i + i0)|^2 d\Omega, \quad (3.1)$$

where $\mathcal{V}$ is a quantization volume. Here we keep only the Rayleigh channel and assume that the atomic system is described by the same ground state g before and after the scattering process, which includes the averaging over initial and sum over final Zeeman states. The initial energy of the entire system E_i is given by $E_i=E_g+\hbar\omega$, where E_g is the ground-state energy, and the incoming and outgoing photons have the same frequency $\omega'=\omega$, such that Q_0 is a function of only one frequency $Q_0=Q_0(\omega)$. We consider below the simplest relevant example of an ensemble of "two-level" atoms, which have only one sublevel in its ground state and three Zeeman sublevels in its excited state, such that $F_0=0$ and $F=1$ and in an isotropic situation the total cross section does not depend on the momentum direction and polarization of the incoming photon. We will also ignore any recoil effects in the scattering process and consider the positions of the atoms in a classical approximation, which takes atomic scatterers to be stationary objects fixed and randomly distributed in the space.

For a many-particle system consisting of two-level atoms the vector properties of the electromagnetic interaction can be taken into consideration, and this is essential for reliable comparison of a microscopic description with predictions of the macroscopic self-consistent model. In the literature, the cooperative or anticooperative effects in many-particle Dicke-type systems are often discussed in a more simple but convenient model, where the vector properties of electromagnetic field are ignored and the field is considered in a scalar wave approximation [19,20]. Our analysis, which goes beyond the scalar model, addresses real physical systems where the description of the short-range interatomic interaction is properly done. This interaction naturally arises from the fundamental atom-field interaction Hamiltonian and, as we shall further show, is very important for a correct evaluation of the T matrix and the resolvent operator.

The T matrix is expressed by the total Hamiltonian $H=H_0+V$ and by its interaction part V as

$$T(E) = V + V\frac{1}{E-H}V. \quad (3.2)$$

In the rotating wave approximation the internal resolvent operator contributes to Eq. (3.1) only by being projected on the states consisting of single atom excitation, distributed over the ensemble, and the vacuum state for all the field modes. Defining such a projector as P, the projected resolvent,

$$\tilde{R}(E) = P\frac{1}{E-H}P, \quad (3.3)$$

performs a $3N\times 3N$ matrix, where N is the number of atoms. For the dipole-type interaction between atoms and field this projected resolvent can be found as the inverse matrix of the following operator:

$$\tilde{R}^{-1}(E) = P\left(E - H_0 - VQ\frac{1}{E-H_0}QV\right)P, \quad (3.4)$$

where the complementary projector $Q=1-P$, operating in the self-energy term, can generate only two types of intermediate states: a single photon plus all the atoms in the ground state and a single photon plus two different atoms in the excited state and the others are in the ground state. For such particular projections there is the following important constraint on the interaction Hamiltonian $PVP=QVQ=0$, which is apparently valid for the dipole-type interaction $V=-\Sigma\mathbf{d}^{(a)}\mathbf{E}_a$, where $\mathbf{d}^{(a)}$ is a dipole operator of an ath atom and $\mathbf{E}_a$ is the microscopic displacement field at the point where the atom is located, see Eqs. (2.1) and (2.2). Due to this constraint the series for the inverse resolvent [Eq. (3.4)] is expressed by a finite number of terms, which would not be the case in a general situation. The explicit expression of the matrix of the inverse resolvent is given in Appendix B.

The explicit description of the dipole interaction for atoms randomly distributed in space and separated by arbitrary distances has been the subject of various discussions in the literature, see Refs. [21–25]. This interaction concerns the

structure of the self-energy matrix contributing to the resolvent operator, see Appendix B, which includes the dipoles with a retardation zone and is crucially important for rigorous analysis of the Dicke-type systems. In our case the analytical behavior of the resolvent operator $\tilde{R}(E)$ gives a relevant theoretical criterion to discriminate the following two limiting situations for light interaction with disordered atomic system: (i) at low densities the light transport is properly described by the mechanism of successive scattering and light diffusion. The resolvent as well as the T matrix can be expressed by a series of partial contributions for a set of subsequent scattering events. Weak deviation from the standard diffusion law (which assumes the absence of correlations and interference) is visible, for example, via the coherent backscattering channel. (ii) At high densities the interaction of atoms with light becomes strongly collectivized and the resolvent has a resonance structure revealing the spectrum of collective excitations. In this situation each resonance pole of the resolvent indicates an atomic state built as a certain entangled superposition for single excitation distributed among all the atomic dipoles. The band of such states can be considered as an excitation zone created by the disordered atomic system and the spectral locations of the resonances as well as their lifetimes are extremely sensitive to any particular configuration of the atomic spatial distribution. From the optical point of view such a resonant band can be considered as a microcavity constructed by the spatial distribution of the system of atomic scatterers.

The resolvent $\tilde{R}(E)$ can be numerically calculated and, for an atomic system consisting of a macroscopic number of atoms, when $N \gg 1$, the microscopically calculated cross section [Eq. (3.1)] can be compared with the Debye-Mie theory results [Eq. (2.14)]. It is important to note that neither the microscopic nor the self-consistent approach uses any fitting parameters. Compared with the macroscopic result, the essential difference between the two approaches is that in the microscopic approach *any collective atomic excitations* can contribute, which also include *any type of entangled states either cooperative or anticooperative*. One can then expect, for some ranges of parameters, significant differences in their predictions for the cross section and for the time evolution of the system fluorescence. Finally, we point out that the time dependence of the fluorescence signal is built up here via the Fourier expansion of the outgoing photon wave packet with the S-matrix formalism.

IV. RESULTS AND DISCUSSION

Below we consider the spectral dependence of the cross sections, calculated in both the self-consistent mesoscopic model and in a microscopic approach. Our central idea is to follow how this dependence is modified when the dimensionless density of atoms $n_0\lambda\!\!\!^{-3}$ is varied from smaller to greater values. We also explore a similar comparison but for variations in the radius of the spherical sample. In these variations, other basic atomic properties, such as the bare resonance frequencies and radiative decay rates, are considered to remain fixed.

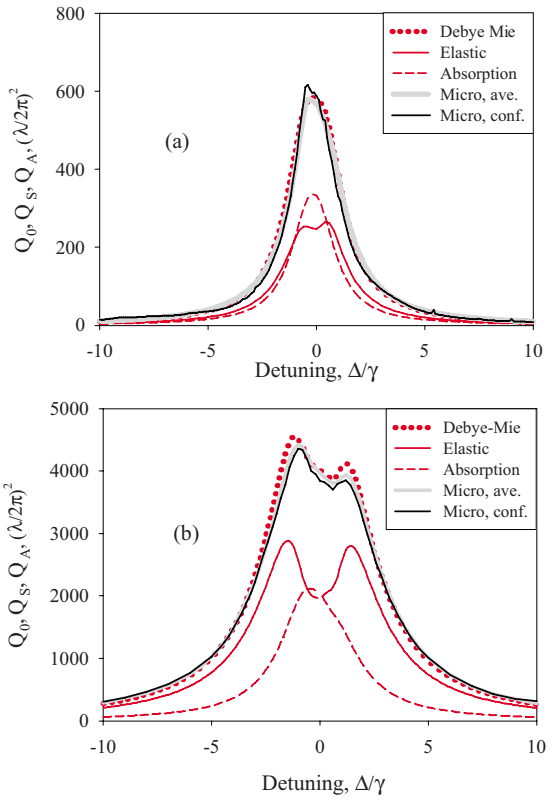

FIG. 3. (Color online) The spectral dependence of the total Q_0, elastic Q_S, and "absorption" Q_A cross sections for atomic samples of size (a) $a=10\lambda\!\!\!^{-}$ and (b) $a=25\lambda\!\!\!^{-}$ and density $n_0\lambda\!\!\!^{-3}=0.02$. The configuration averaged microscopic result, shown as a wide solid line, is evidently the same as the data taken for particular atomic configuration, shown as a black line. The results of a mesoscopic self-consistent approach, as labeled in the legend, reproduce the exact microscopic spectra.

In Fig. 1 we reproduce such a spectral dependence when the density of atoms is small, $n_0\lambda\!\!\!^{-3}=0.02$. For a spherical and uniform density of ultracold Rb atoms, this corresponds to an atom density of 1.3×10^{12} atoms/cm^3, which is a density readily achievable in a magnetic or optical dipole trap. In the figure there are results representing the total scattering cross section for the microscopic and Debye-Mie treatments. In addition, it is possible in the Debye-Mie theory to separate out the elastic and inelastic parts of the cross section; these are shown as the lower peak cross-section graphs in Fig. 3. For the total cross-section results in Fig. 3, we see that is excellent agreement between the Debye-Mie and microscopically calculated data. We further note that the microscopic result is insensitive to configuration averaging (shown as the gray solid curve) over random spatial atomic distributions. We point out that deviation from the averaged dependence of the data calculated for any particular configuration is less as the total number of atoms N is greater and, within the numerical accuracy of our calculations, vanishes as the macroscopic limit ($N\to\infty$) is approached. This is emphasized in the microscopically calculated dependencies of Fig. 1 for greater N in case (b) the deviation from the configuration averaged result is less visible than in case (a) relating to smaller N. Finally, it is noteworthy that the effects of mac-

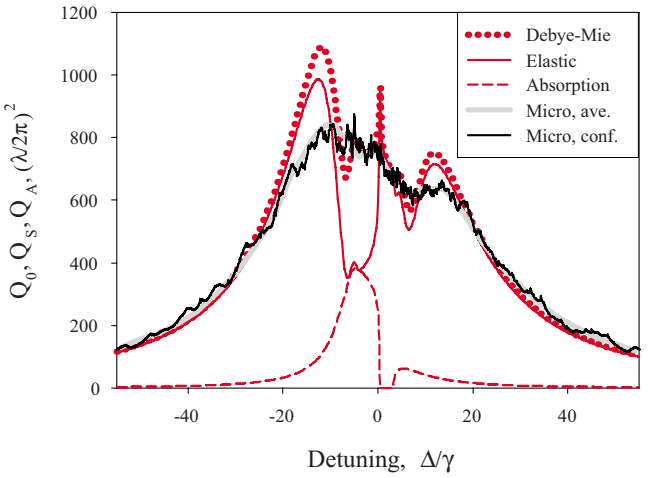

FIG. 4. (Color online) Same as Fig. 3 but for a sample size $a=10\lambda$ and density $n_0\lambda^3=0.5$. The results of the self-consistent mesoscopic approach, as labeled in the legend, perceptibly differ from the microscopic spectra. In turn, the microscopic calculation given for a particular configuration (black curve) indicates a microcavity structure generated by the resolvent poles.

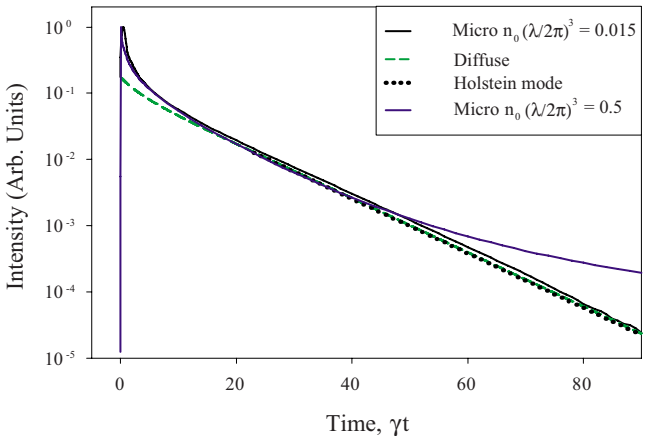

FIG. 5. (Color online) Time-dependent fluorescence decay for samples of different densities and with nearly equal optical depths. The dilute system has a sample radius $a=27\lambda$ and density $n_0\lambda^3=0.015$, and for the dense system these characteristics are given by $a=5\lambda$ and $n_0\lambda^3=0.5$.

roscopic electrodynamics are important even at relatively low densities $n_0\lambda^3\sim 0.02$. For example, at the point of its maximum the Debye-Mie cross section is larger than $2\pi a^2$ because of refraction when ϵ' differs from its vacuum value. According to the Fresnel boundary conditions, which are asymptotically valid for a sample with a planar boundary, the surface reflection is always stronger as the difference between the refractive indices of the sample and the external medium is larger. The agreement between microscopic and macroscopic approaches supports the idea that at these densities mainly cooperative modes, which allow the macroscopic Maxwell description, contribute to the scattering process. As a consequence of this point, the long term time dynamics of the fluorescence signal can be well approximated by a Holstein-type mode, which is typical for dilute atomic systems [26]. We have explored this spectral and temporal behavior and find that it is well verified by our numerical simulations done for atomic ensembles of different sizes and consisting of different numbers of atoms.

While varying the density to greater values $n_0\lambda^3\sim n_c\sim 0.09$ the solution of the self-consistent Eq. (2.9) turns the permittivity to negative values in a part of the spectrum where $\epsilon'<0$ and $\epsilon''=0$. As is well known in, e.g., plasma physics [11] the negative permittivity can be associated with a forbidden spectral zone, where the radiation cannot penetrate inside the system and can exist only in the form of a surface light-matter wave, see comment in Sec. II B. In the limit of even higher density samples, the light undergoes mainly surface scattering and the absorption (incoherent and diffusion scattering) channels suppressed. This is illustrated in Fig. 4 by those spectral dependencies of the cross section, which were calculated in the Debye-Mie model for $n_0\lambda^3=0.5$. In contrast with similar results in Fig. 3 the contribution of the elastic channel now dominates such that a smaller portion of light can penetrate the sample. As a consequence, it is expected that fewer atomic excitations should contribute to the time-dependent fluorescence decay and the self-consistent model predicts an even faster decay than would take place in a similar, but more dilute, system.

The situation can be differently posed if it is considered from a microscopic point of view. Then such a dense atomic vapor can be described as a microcavity system built up in an environment of randomly distributed atomic scatterers. Any distribution creates a specific quantization problem for the incoming field, whose mode structure can be properly defined in terms of standard scattering theory, see Sec. III. The main difficulty for the quantization procedure is description of the complicated structure of the resonance states. The resonances are described by the resolvent poles and can be specified by various superpositions of atomic states, which transform the inverse projected resolvent [Eq. (3.4)] to diagonal form. The microcavity structure manifests itself by the appearance of spectrally narrow structure in the scattering spectrum and the scattering process becomes extremely sensitive to the spatial configuration of atomic scatterers, as illustrated in Fig. 4. Some of these resonance states have a subradiant nature and manifest themselves via significantly slowed long-time decay of the fluorescence in comparison with a classical Holstein mode. Figure 5 illustrates the difference in the fluorescence decay for dilute and dense atomic systems initially excited by a short probe pulse. The external parameters for the systems are such that the optical depth for each of the systems is nearly the same. In Fig. 5, four cases are illustrated. The dashed curve represents a solution to the diffusion equation for the sample geometry and optical characteristics. The curve labeled with shorter dashes represents the longest-lived (Holstein) mode for identical conditions. Third, the time evolution of the intensity, extracted through exact microscopic calculations in the dilute case, is well described by a diffuse Holstein-type mode evaluated via the sample macroscopic characteristics. Each of these three cases are very similar, illustrating that the longest time asymptotic behavior of the intensity, for a dilute sample, is well described by a diffusion picture. However, for the dense system there is evident very strong deviation of the asymptotic behavior from such behavior. Such a deviation should be asso-

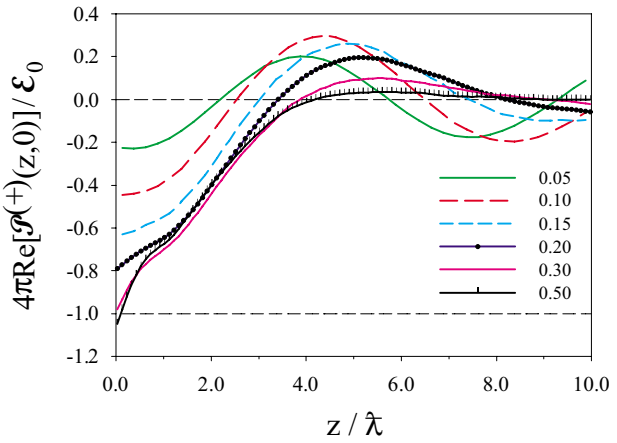

FIG. 6. (Color online) The mesoscopically averaged polarization wave $\mathcal{P}^{(+)}(\mathbf{r}_\perp,z,t)|_{\mathbf{r}_\perp=0,t=0}$ distributed along the central part of a cylindrical atomic sample with radius $R=15\lambda$ and length $L=10\lambda$. The frequency of the driving field is tuned by $+2\gamma$ from atomic resonance to adjust the polarization response to be in opposite phase with the electric field and the plotted data relate to the time of maximal oscillation at the sample boundary. The graphs reproduce the real part of the positive frequency component and are normalized to the amplitude $\mathcal{E}_0$ of the driving field at the sample boundary. While varying the density $n_0\lambda^3$ from lower to higher values, as indicated in the figure legend, one can attain the conditions when the displacement field will be also in opposite phase with the electric field (horizontal dashed line at -1), which is macroscopically described by regime of negative dielectric constant.

ciated with the presence of subradiant resonance states in the resolvent poles.

It is interesting that the discrepancy between the dependencies of Figs. 4 and 5, which were calculated based on different approaches, is not dramatically large. This indicates that some effects of macroscopic electrodynamics do not completely wash out in the considered dense and lossless atomic system. The macroscopic Maxwell equations operating with the mesoscopically averaged electric and displacement fields are partly valid and some of the predictions of the self-consistent model are correct and can be verified. The knowledge of the resolvent operator allows us to describe the dynamics of a weak coherent excitation, which can be approximated as a superposition of the vacuum and single excitation states. Thus one can apply the microscopic approach for calculation of the dynamics of the material wave associated with the mesoscopically averaged dipole polarization in such a disordered system. Instead of spherical geometry we shall consider an example of a cylindrical sample with large radius, such that the dipole polarization near the central part of the sample would asymptotically approach a one-dimension system. The relevant example is shown in Fig. 6 where the polarization wave is reproduced for different densities and for the conditions when the dipoles' dynamics is in opposite phase with the driving field. This is generated through a small detuning of the driving mode to the high-frequency side of atomic resonance, which is equal to $+2\gamma$ for the plotted graphs. It is evidently from the shown dependencies that at low densities the polarization wave indicates normal behavior and propagates inside the sample. But at higher densities the macroscopic polarization transforms to the surface wave located near the sample boundary. The magnitude of the polarization can be so high that the displacement field can be also in opposite phase with the driving wave that displays the situation of negative dielectric constant. However this effect is evidently weaker than what is predicted by the self-consistent model. This also justifies that the cooperatively responding collective states of atomic dipoles only partly contribute to the actual sample polarization and the contribution of the resonances built by entangled subradiant states rises with the density.

The possible connection between subradiant states as an atomic physics analog to light localization, usually discussed in terms of multiple wave scattering, suggests evolution with density of the qualitative scattering properties of the atomic gas. The characteristics discussed here, such as the spectral dependence of the sample cross section and the time-dependent fluorescence, describe how the system in equilibrium responds to optical excitation near the atomic resonance transition. The atomic transition is dressed by cooperative dipole-field interactions and at higher densities, the disordered atomic system reveals a microcavity structure. Such a microcavity has unique properties for any particular configuration and its mode splitting is competitive with the mode decay rate. The configuration-sensitive resonance structure of the spectral cross section manifests itself in those conditions when the self-consistent permittivity becomes negative in part of the spectrum. The description of the atomic system with the macroscopic Maxwell theory preferably yields surface scattering of light in this case. More precise microscopic description shows that part of the excitation can in fact penetrate the atomic system and lead to a long time decay of the fluorescence signal.

V. SUMMARY AND CONCLUSIONS

In this paper we have presented a comparative study of two alternative theoretical descriptions of light scattering from an ultracold, but not quantum degenerate, atomic sample. The investigation is specifically focused toward understanding some aspects of the scattering processes that can occur and how they vary as the atomic density is varied from low values to levels where the mean separation between atoms is on the order of λ. One of the treatments is a self-consistent approach based on the Debye-Mie theory of the spectral response of an atomic system, while the other is a fully quantum-posed description of the weak-field light-scattering dynamics. Our main findings are: (a) for lower atomic densities, the two approaches give nearly identical results for the light-scattering cross section from a spherical sample of atoms; (b) for higher atomic densities a spectral distribution of narrow resonances appear in the quantum-posed results. The distribution depends on the particular atomic spatial configuration and smooths upon configuration averaging. Such resonances do not appear in the self-consistent treatment; (c) under conditions where such microcavity resonances appear, the average time evolution of the emergence of a single-photon wave packet from the sample is considerably slowed in comparison with the expected

spherically symmetric diffusive decay mode under nearly identical physical conditions; (d) when considering a one-dimension system of high density, we find that penetration of incident radiation is suppressed, and a corresponding polaritonic excitation appears in the vicinity of the sample boundary, which is also predicted by macroscopic approach. Of these results, the appearance of microcavity-type resonances is most intriguing and may bear importantly on the question of the existence of subradiant and super-radiant configurations in such systems. Taken together, even the limited subset of our initial results as presented here suggest that the quantum optics of denser and ultracold atomic systems represent an intriguing and rich area for future investigation

ACKNOWLEDGMENTS

We appreciate the financial support by the Russian Foundation for Basic Research (Grant No. RFBR-08-02-91355), the National Science Foundation (Grant No. NSF-PHY-0654226), and INTAS (Project No. 7904).

APPENDIX A: THE SELF-ACTION AND SELF-CONTACT TERMS

The contribution of the self-contact interaction, extracted from the microdisplacement field, and of the self-action term into the dynamics of the selected dipole is given by

$$\dot{\hat{d}}_j^{(a,+)}(t) = \cdots + \frac{i}{\hbar}[\hat{H}_{\rm self}(t), \hat{d}_j^{(a,+)}(t)] - \frac{i}{\hbar}\frac{4\pi}{\mathcal{V}}\sum_s e_{si}[\mathbf{e}_s \mathbf{d}^{(a,-)}(t)] \times [d_i^{(a,-)}(t), d_j^{(a,+)}(t)] - \frac{i}{\hbar}[d_i^{(a,-)}(t), d_j^{(a,+)}(t)] \times \frac{4\pi}{\mathcal{V}}\sum_s e_{si}[\mathbf{e}_s \mathbf{d}^{(a,+)}(t)], \tag{A1}$$

where the dots indicate all the terms associated with the transverse electric field and interaction with other dipoles, which are discussed in the main text of the paper.

The self-action term (dipolar self-energy) arises as a result of unitary transformation of the fundamental atom-field Hamiltonian to the long-wavelength dipole representation, see Ref. [12] for details. It is given by

$$\hat{H}_{\rm self}(t) = \frac{2\pi}{\mathcal{V}}\sum_s [\mathbf{e}_s \mathbf{d}^{(a)}(t)]^2, \tag{A2}$$

and its commutator with the dipole operator in Eq. (A1) is expressed as follows:

$$\frac{i}{\hbar}[\hat{H}_{\rm self}(t), \hat{d}_j^{(a,+)}(t)] = \frac{i}{\hbar}\frac{2\pi}{\mathcal{V}}\sum_s e_{si}[\mathbf{e}_s \mathbf{d}^{(a)}(t)][d_i^{(a,-)}(t), d_j^{(a,+)}(t)] + \frac{i}{\hbar}[d_i^{(a,-)}(t), d_j^{(a,+)}(t)]\frac{2\pi}{\mathcal{V}}\sum_s e_{si}[\mathbf{e}_s \mathbf{d}^{(a)}(t)]. \tag{A3}$$

As one can see there is no exact compensation of the self-contact interaction by the self-action term. But while averaging the equation of motion and while assuming the weak excitation by external field, it is relevant to ignore the Heisenberg dynamics of the commutator of the dipole's operators and approximate it by c number in accordance with the following rule:

$$[d_i^{(a,-)}(t), d_j^{(a,+)}(t)] \to -\delta_{ij}\frac{|d_{F_0F}|^2}{3(2F_0+1)}, \tag{A4}$$

where F_0 and F are, respectively, the total angular momenta of the ground and excited states of the considered atomic transition and d_{F_0F} is the reduced matrix element of the dipole moment. We apply this approximation with the arguments similar to those, which were originally done for the spin subsystems in Ref. [27]. Then one straightforwardly obtains

$$\dot{\hat{d}}_j^{(a,+)}(t) = \cdots + 0. \tag{A5}$$

It is also noteworthy that neither of the terms make any contribution into the dynamics of real observables (not frequency part) of an atomic dipole.

APPENDIX B: THE MATRIX OF THE INVERSE RESOLVENT

The inverse resolvent $\tilde{R}^{-1}(E)$ can be expressed in terms of its self-energy part as follows:

$$[\tilde{R}^{-1}(E)]_{nn'}^{(ab)} = (E - \hbar\omega_0)\delta_{ab}\delta_{nn'} - \Sigma_{nn'}^{(ab)}, \tag{B1}$$

where the first term is the nonperturbed diagonal contribution and the second term performs the matrix of the self-energy part $\Sigma_{nn'}^{(ab)}$. This matrix, given by the last term in the brackets of Eq. (3.4), is symmetric over the indices of the atomic pairs a,b such that $\Sigma_{nn'}^{(ab)} = \Sigma_{nn'}^{(ba)}$. While calculating the self-energy matrix we apply the standard pole or "on-shell" approximation, similar to the Wigner-Weiskopf approach for single atom spontaneous emission, and substitute $E = \hbar\omega_0$ (i.e., undressed energy of the excited state with assumption that $E_g = 0$) in it that means $\Sigma_{nn'}^{(ab)}(E) \approx \Sigma_{nn'}^{(ab)}(\hbar\omega_0) \equiv \Sigma_{nn'}^{(ab)}$.

For $a = b$, i.e., for any ath atom, this matrix is trivially diagonal in the basis of the atomic excited states $|n\rangle$ and $\Sigma_{nn'}^{(ab)}|_{a=b} = \Sigma^{(a)}\delta_{nn'}$, where

$$\Sigma^{(a)} = \hbar\Delta_{\rm L} - i\hbar\frac{\gamma}{2}, \tag{B2}$$

and it is independent of a. Here $\Delta_{\rm L}$ is the standard Lamb shift, which approaches infinity in the long-wavelength dipole representation, and it should be renormalized into the physical value of the transition frequency. The second term defines the natural half-linewidth $\gamma/2$ of the excited state resonance for an isolated atom.

For $a \neq b$ the matrix elements are identical for each pair, and we can simplify our notation by removing the atom's indices and denoting $\Sigma_{nn'}^{(ab)} \Rightarrow \Sigma_{nn'}$, where the quantum numbers n and n' should be associated with the excited states of

different atoms in a pair. For the simplest situation of a ^1P configuration of the atomic excited state the matrix elements $\Sigma_{nn'}$ are given by

$$\Sigma_{nn} = -i\hbar\frac{\gamma}{2}\left[h_0^{(1)}(k_0 r) + \left(-\frac{1}{2}\right)^{|n|}\sqrt{\frac{4\pi}{5}}h_2^{(1)}(k_0 r)Y_{20}(\theta,\varphi)\right] \tag{B3}$$

if $n'=n$ and

$$\Sigma_{nn'} = -i\hbar\frac{\gamma}{2}(-1)^n\sqrt{\frac{3\pi|n'-n|}{5}}h_2^{(1)}(k_0 r)Y_{2n'-n}(\theta,\varphi) \tag{B4}$$

if $n' \neq n$, where $n', n = 0, \pm 1$, $k_0 = \omega_0/c = \lambda\!\!\!^{-1}$, see [21,23]. Here $h_L^{(1)}(k_0 r)$ are spherical Hankel functions of the first kind and $Y_{LM}(\theta,\varphi)$ are spherical harmonics. The relative coordinates of the selected atomic pair are defined in a spherical frame with separation r and solid angle $\Omega = \theta, \varphi$

[1] C. J. Pethick and H. Smith, *Bose-Einstein Condensation in Dilute Gases*, (Cambridge University Press, Cambridge, UK, 2002).

[2] R. Wester, S. D. Kraft, M. Mudrich, M. U. Staudt, J. Lange, N. Vanhaecke, O. Dulieu, and M. Weidemüller, Appl. Phys. B: Lasers Opt. **79**, 993 (2004).

[3] R. M. Camacho, C. J. Broadbent, I. Ali-Khan, and J. C. Howell, Phys. Rev. Lett. **98**, 043902 (2007).

[4] D. Bouwmeester, A. Ekert, and A. Zeilinger, *The Physics of Quantum Information* (Springer-Verlag, Berlin, 2000).

[5] R. H. Dicke, Phys. Rev. **93**, 99 (1954).

[6] P. W. Anderson, Phys. Rev. **109**, 1492 (1958).

[7] H. Cao, Waves Random Media **13**, R1 (2003).

[8] E. Akkermans and G. Montambaux, *Mesoscopic Physics of Electrons and Photons* (Cambridge University Press, New York, 2007).

[9] P. Sheng, *Introduction to Wave Scattering, Localization, and Mesoscopic Phenomena* (Academic Press, San Diego, 1995).

[10] A. Gero and E. Akkermans, Phys. Rev. A **75**, 053413 (2007).

[11] E. M. Lifshits and L. P. Pitaevskii, *Course of Theoretical Physics: Statistical Physics*, (Pergamon, Oxford, 1980), Part II; L. D. Landau and E. M. Lifshits *Electrodynamics of Continuous Media* (Pergamon Press, Oxford, 1981).

[12] C. Cohen-Tannoudji, J. Dupont-Roc, and G. Grynberg, *Atom-Photon Interactions. Basic Processes and Applications* (John Wiley & Sons, Inc., New York, 1992).

[13] M. Born and E. Wolf, *Principles of Optics* (Pergamon Press, New York, 1964).

[14] S. Prasad and R. J. Glauber, Phys. Rev. A **61**, 063814 (2000).

[15] The local-field (Lorentz-Lorenz) correction has an order of magnitude of the longitudinal electric field created by a dipole of the medium at a distance of the average interatomic separation in the medium. This correction takes place when the self-action and the self-contact interaction in the dipole's dynamics are eliminated, see Appendix A. The local-field correction approximates the longitudinal interaction with other proximal dipoles via considering the selected dipole as located in a small spherical cavity inside the homogeneous dielectric medium.

[16] R. J. Glauber and M. Lewenstein, Phys. Rev. A **43**, 467 (1991).

[17] H. Fu and P. R. Berman, Phys. Rev. A **72**, 022104 (2005).

[18] O. Morice, Y. Castin, and J. Dalibard, Phys. Rev. A **51**, 3896 (1995).

[19] M. Rusek, J. Mostowski, and A. Orlowski, Phys. Rev. A **61**, 022704 (2000); F. A. Pinheiro, M. Rusek, A. Orlowski, and B. A. van Tiggelen Phys. Rev. E **69**, 026605 (2004).

[20] A. A. Svidzinsky, J. T. Chang, and M. O. Scully, Phys. Rev. Lett. **100**, 160504 (2008).

[21] V. B. Beresteskii, E. M. Lifshits, and L. P. Pitaevskii, *Course of Theoretical Physics: Quantum Electrodynamics* (Pergamon Press, Oxford, 1981).

[22] M. J. Stephen, J. Chem. Phys. **40**, 669 (1964).

[23] D. A. Hutchinson and H. F. Hameka, J. Chem. Phys. **41**, 2006 (1964).

[24] R. H. Lehmberg, Phys. Rev. A **2**, 883 (1970).

[25] P. W. Milonni and P. L. Knight, Phys. Rev. A **10**, 1096 (1974).

[26] G. Labeyrie, E. Vaujour, C. A. Muller, D. Delande, C. Miniatura, D. Wilkowski, and R. Kaiser, Phys. Rev. Lett. **91**, 223904 (2003).

[27] T. Holstein and H. Primakoff, Phys. Rev. **58**, 1098 (1940).